



Volume 121

2023

p-ISSN: 0209-3324

e-ISSN: 2450-1549

DOI: <https://doi.org/10.20858/sjsutst.2023.121.4>

Journal homepage: <http://sjsutst.polsl.pl>



---

**Article citation information:**

Cieślak, K., Płonka, S. Modeling of rough rotary milling of crankshaft pins. *Scientific Journal of Silesian University of Technology. Series Transport*. 2023, **121**, 45-61. ISSN: 0209-3324. DOI: <https://doi.org/10.20858/sjsutst.2023.121.4>.

Kacper CIEŚLAR<sup>1</sup>, Stanisław PŁONKA<sup>2</sup>

## MODELING OF ROUGH ROTARY MILLING OF CRANKSHAFT PINS

**Summary.** The development of the modern automotive industry requires a quick adaptation of new production methods. This is possible thanks to software capable of simulating manufacturing processes. The paper discusses the modeling of the machining operation of a crankshaft's crankpins for a diesel engine with the use of the planetary milling method. i.e., modeling of milling operation when a disc milling cutter, having its cutting inserts directed inwards, is performing rotary motion, and at the same time, the axis of this milling cutter circulates around the axis of a machined crankpin. For this purpose, a geometrical model of the machining of the crankshaft's crankpin has been developed. Based on the design documentation of the crankshaft of the 4C90 type diesel engine and the documentation of the Steyr internal disc milling cutter, their CAD models have been developed, and the both models were linked together with suitable kinematic dependencies. In the next step, the crankpin having a length of 25 mm was divided by planes (in quantity  $l_p=21$ ) into 1.25 mm sections. On the main cutting edge of two cutting inserts of the disc milling cutter, points were marked at intersection locations with these planes. Using the Inventor 2016 system, twelve spline curves have been generated for each plane because each plane intersects 12 cutting inserts mounted in cassettes positioned around the circumference of the body of the disc milling cutter. Next, the spline curves were brought to a common coordinate system, rotating them at an angle resulting from the positioning of the cassettes

---

<sup>1</sup> Faculty of Mechanical Engineering, University of Bielsko-Biala, Willowa 2 Street, 43-309 Bielsko-Biala, Poland. Email: [kcieslar@ath.bielsko.pl](mailto:kcieslar@ath.bielsko.pl). ORCID: <https://orcid.org/0000-0001-9552-025X>

<sup>2</sup> Faculty of Mechanical Engineering, University of Bielsko-Biala, Willowa 2 Street, 43-309 Bielsko-Biala, Poland. Email: [splonka@ath.bielsko.pl](mailto:splonka@ath.bielsko.pl). ORCID: <https://orcid.org/0000-0001-7586-7854>

with cutting inserts in the body of the disc milling cutter. Prepared in such a way, spline curves were written in dwg format, which allowed for trimming of the spline curves at the circle with a radius of  $r_{cp} = 27.90$  mm, corresponding to the radius of the crankpin after milling, considering grinding allowance ( $\varnothing 55h6 + 0.80$  mm grinding allowance). As a result, it enabled to leave sections of the arcs tangential to the diameter  $\varnothing 55.80$  mm and, in such a way, generate the outline of the shape of the crankpin using the REGION command for 21 cross-sections. The outline of the cylindricity of the crankpin was obtained using the strategy of outlines of the roundness, which were generated earlier; this strategy consisted in the collection of 360 points on the circumference of 21 mutually parallel sections cut by planes perpendicular to the axis of the crankpin. To determine the effects of the circular feed rate of the circulating move of the axis of rotation of the internal disc milling cutter on the accuracy of the machining, simulations of the shape of the crankpin were performed for three values of the feedrate:  $v_f = 1200$  mm/min;  $v_f = 2100$  mm/min and  $v_f = 3000$  mm/min. The spline curves with a determined (depending on the duration of the simulation) number of points: 3500, 2100 and 1409 were obtained for each simulation. The calculated cylindricity deviation for the feedrate  $v_f = 1200$  mm/min amounted to  $CYLrck = 0.2272$  mm, for the feedrate  $v_f = 2100$  mm/min –  $CYLrck = 0.2406$  mm, while for the feedrate  $v_f = 3000$  mm/min –  $CYLrck = 0.2929$  mm.

**Keywords:** modeling of machining, crank shaft, internal rotary milling

## 1. INTRODUCTION

The development of the modern automotive industry requires constant improvements. This is caused by the desire to increase the power of internal combustion engines while reducing the pollution they emit. It should be remembered that the effect of the design phase will have an impact on the operational process, including an increased probability of unexpected engine failures resulting from damage to its various components [18, 19]. Modeling with the use of computer programs makes it possible to accelerate the implementation of new technical solutions, e.g. by analyzing the production of crankshafts, it can be concluded that the technological processes of their machining are very complex, and by performing machining simulation, the process can be improved even before its actual implementation. The crankshaft belongs to one of the most responsible structural components of the combustion engine, participating in the conversion of reciprocating movement of the piston into rotational movement, and at the same time, it repeatedly transfers quite high, periodically acting loads [17]. Due to the imposed requirements and shape of the crankshafts, their manufacturing processes must meet high qualitative requirements. The choice of manufacturing process depends mainly on production volumes and the overall dimensions of the crankshaft, and, to a lesser extent, on the kind of blank. In the last century, in the course of unit and small series production, the main journals and the crankpins were machined by turning operations, wherein the crankpins were generally machined with the use of special machining fixtures. On the other hand, in cases of mass volume production, machining of the crankpins was carried out using the three-shaft method on a special automatic lathe, consisting of simultaneous turning of all crankpins [17]. Such a method was used to machine the journals of a crankshaft with four cranks, produced as a casting from spheroidal cast iron, and mounted in the 899 ccm passenger cars of the Seicento brand. Nowadays, in the production of the crankshafts, due to production

efficiency, in the case of rough and shaping machining of both the main journals and the crankpins, external rotary milling or internal rotary milling systems are used, or relatively, planetary milling with special disc milling cutters having cutting inserts mounted mechanically [2, 7-9, 11]. Except for the above-mentioned methods of rotary and planetary milling, turn broaching with the use of flat broaches, or more often, turn-turn broaching operations, are used in the mass production of the crankshafts. The second solution, due to its kinematic features, is called a turning & broaching operation (rotary broaching) [2, 5, 6]. The shaping operation of the main journals of the 1.3 SDE diesel engine's crankshaft, performed in the Bielsko-Biala plant, is an example of the turning & broaching operation with the use of rotary broaches. To machining of the main journals in course of mass production and small-volume production, turning machining on CNC center lathes was generally used, whereas machining of the crankpins was performed using internal rotary milling or planetary milling operations. Nowadays, machining of both the main journals and the crankpins is performed most frequently in the course of internal planetary milling, while basing on already machined main journals, one machines alternatively the crankpin, and next the main journal, changing position of the angular prop. In case of unit or prototype production, the crankshafts can be manufactured from rolled bars in milling-turning operations on WFL turning-milling centers with 5 axes controlled [10].

The main objective of rough machining is to provide a large depth of cutting and, therefore, high productivity. Less attention is paid to geometrical accuracy and surface quality as obtained in subsequent operations of shaping and finishing, i.e., in operations of shaping and grinding, and next, in the case of mass production, the most often, oscillating superfinishing with abrasive foils.

Presentation of geometrical modeling stages of planetary milling operation of crankshaft crankpins and determination of the effects of the circular feedrate of the circulating movement of the axis of rotation of the internal disc milling cutter (rotational speed of the eccentric housing  $n_{om}$ ) on machining accuracy (simulation) of shape of the crankpin are the main objectives of this study. Therefore, the simulations were carried out for three values of circular feed rate  $v_f$  (values of rotational speed of the eccentric housing  $n_{om}$ ):  $v_f = 1200$  mm/min ( $n_{om} \approx 1,70$  rpm);  $v_f = 2100$  mm/min ( $n_{om} \approx 2,98$  rpm); and  $v_f = 3000$  mm/min ( $n_{om} \approx 4,26$  rpm).

## 2. METHOD OF PLANETARY MILLING OF THE CRANKSHAFTS

A die forging from 42CrMo4 steel was used as a semifinished product in the production of the crankshaft with 4 cranks for the 4C90 type diesel engine. In the study, one analyzed the rough machining using the method of planetary milling of selected crankpins of this engine using an internal disc milling cutter on a special numerically controlled Steyr FKP-20/1 milling machine [9]. The machining scheme of the crankpin performed by planetary milling is shown in Figure 1, while individual machining stages of the crankpin are shown in Figure 2.

Unlike external and internal rotary milling, the crankshaft is at a standstill during planetary milling. The planetary movement is performed by internal disc milling cutter, this movement is composed of rotational movement of the cutter with speed  $n_{mc}$  in rpm, and circulating move with circular feed rate of the axis of rotation (center of symmetry) of milling cutter around axis of machined crankpin with feedrate  $v_f$  in mm/min. In reality, circulating move of axis of rotation of the disc milling cutter around axis of machined crankpin of the crankshaft occurs as result of rotational movement with speed  $n_{om}$  of the eccentric housing together with internal disc milling cutter rotating with speed  $n_{mc}$ .

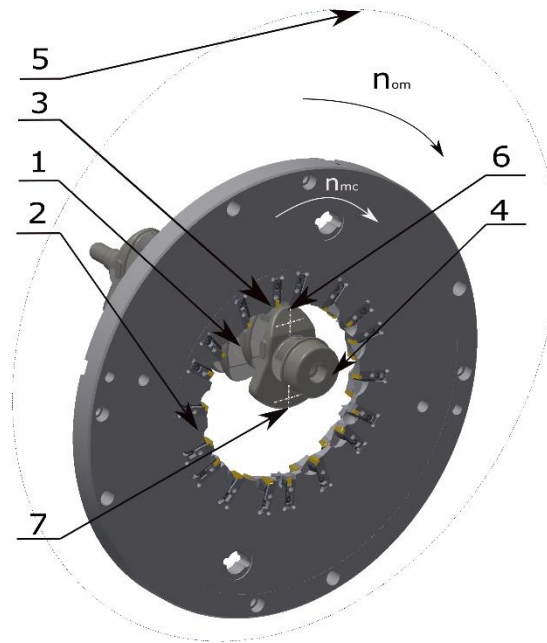


Fig. 1. Scheme of planetary milling of crankshaft's crankpin using internal disc milling cutter:  
 1 – crankshaft of 4C90 type diesel engine with 4 cranks; 2 – internal disc milling cutter;  
 3 – crankpin, 4 – main journal (bearing journal), 5 – eccentric housing, 6 – axis of symmetry  
 of machined crankpin, 7 – axis of rotation of internal disc milling cutter

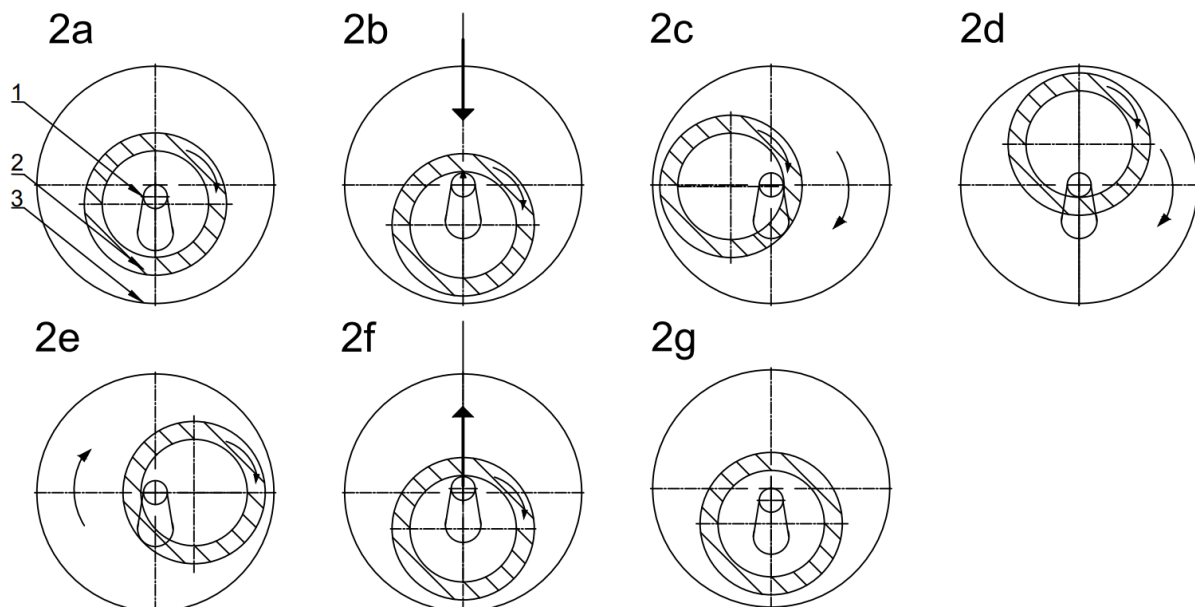


Fig. 2. Machining stages of crankshaft's crankpin during planetary milling:  
 1 – crankpin of the crankshaft, 2 – internal disc milling cutter, 3 – eccentric housing

In the initial position, the axis of symmetry of the crankpin which undergoes the machining, and the axis of rotation of the internal milling cutter, rotating with speed  $n_{mc}$ , are located in the same plane, for instance, a vertical one. The disc milling cutter is moved away from the crankpin (Fig. 2a). In the case of the crankshafts from in-line engines, the axis of symmetry of

the main journal (bearing journal) is also located in the same plane. In such a position, the crankshaft is permanently fixed hydraulically. After fixing the crankshaft in this position, the transversal infeed of the eccentric housing with the incorporated rotating milling cutter is engaged, and the slide of the housing moves until the moment when the center of symmetry of the eccentric housing is located exactly in the axis of the machined crankpin (Fig. 2b). When the slide of the eccentric housing displaces laterally together with the internal disc milling cutter, the cutting inserts located in the rotating cutter are indented into the machined crankpin to a depth corresponding to half of the machining allowance on the diameter of the crankpin anticipated for the machining. Then occurs jamming of the slide of the lateral move of the eccentric housing, rotational move of the housing with speed  $n_{om}$  switches on, and the same, circulating move with circular feed rate of the axis of rotation of the spinning disc cutter switches on. In position as shown in the figure 2c, the crankpin is machined around a circumference corresponding to angle  $90^\circ$ , while in position as shown in the figure 2d, the crankpin is machined around a circumference corresponding to angle  $180^\circ$ . In the position – as in the figure 2e, the crankpin is machined around a circumference corresponding to angle  $270^\circ$ . Displacement of the axis of rotation of the disc milling cutter spinning in the circle with radius  $(r_{mc} - r_{ck})$  around axis of machined crankpin with  $360^\circ$  ensures machining of this crankpin around its full circumference (Fig. 2f). After completion of machining in this position (Fig. 2f), stoppage and return (retraction) of the eccentric housing together with the internal disc milling cutter to the starting position occur. Machining of the crankpin around its complete circumference is carried out owing to the circulating motion at an angle  $360^\circ$  of the axis of rotation of the disc milling cutter spinning with circular feedrate  $v_f$  in mm/min. This feed rate is enforced by rotating with speed  $n_{om}$  eccentric housing, together with the milling cutter spinning with speed  $n_{mc}$  around the axis of machined crankpin.

### 3. METHOD OF GEOMETRICAL MODELING

In general, geometrical modeling based on 3D modeling modules of CAD systems implements Boolean operations on the models that are the subject of the analysis [15, 16]. The models generated in such a way can serve as examples to assess the geometrical accuracy of the machining, modeling traces of the machining, or as a basis for further analyses.

In the case described here, in the first succession, a geometrical model of the crankshaft of 4C90 diesel engine was developed based on its design documentation, and a geometrical model of the internal disc milling cutter was developed based on the design documentation of this cutter published by Steyr. In the next step, using the 3D parametric modeling module of CAD system, the following system has been modeled: internal disc milling cutter, machined crankshaft crankpin. By defining the appropriate geometrical constraints, the mobility of the internal disc milling cutter was determined, i.e.,

- rotational movement with constant speed  $n_{mc}$  together with maintaining the proper direction of this movement (sign of the speed value),
- movement of the axis of rotation along a circular path with radius  $r_{mc} - r_{ck}$  and the feed rate  $v_f$  around the axis of the machined crankpin (this movement is accomplished by rotation of the eccentric housing with speed  $n_{om}$ ).

The tracking function was used during the simulation of the movement of the model to generate paths of movement for the points lying on the main cutting edge of the cutting inserts of the internal disc milling cutter. In order to reproduce machining conditions, the simulation time was restricted because of the determined circular feed rate of the axis of rotation of the internal disc milling cutter, which required its circulation at  $360^\circ$ . The path of motion of the analyzed point in the form of a spline curve is the effect of the tracking during the simulation. In the case discussed here, this curve was exported in native format, and its further analysis was performed in the 2D modeling module of the CAD system. The function of creating an envelope was used to generate a model of the cross-section of the crankpin being machined in the analyzed plane of motion of the point on the cutting edge of the cutting insert of the internal disc milling cutter.

Necessary designations adopted in the model of machining of the crankshaft's crankpin during planetary milling are shown in Figure 3. As a result of circulating movement of the axis of rotation  $M$  of the internal disc milling cutter rotating about the axis of the crankpin  $P$ , the disc cutter, represented by a substitutive cylindrical surface having radius  $r_{mc}$ , all the time is internally tangent to the cylinder with radius  $r_{ck}$ . Axis of rotation of the disc cutter  $M$ , i.e., center of symmetry of the cylinder with radius  $r_{mc}$ , performs a circulating movement around the axis of the crankpin, and simultaneously, around the center of symmetry of the eccentric housing (for this purpose, it moves around a circle having radius  $r_{mc} - r_{ck}$  with feedrate  $v_f$  - Fig. 3). Axis of the crankpins with radius  $r_{ck}$  is shifted relative to the axis of the main journals with a radius  $r_{cg}$  with a crank radius of  $r_w$ .

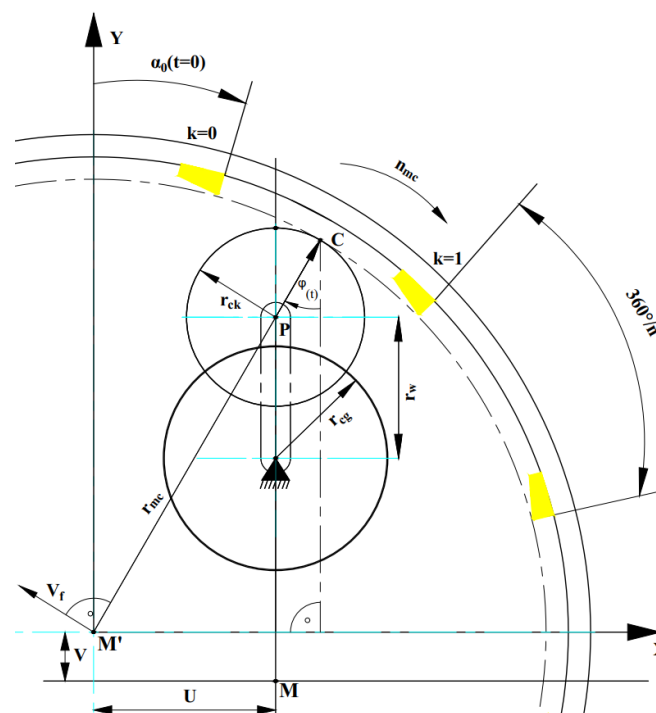


Fig. 3. Machining model of the crankpin during planetary milling with use of an internal disc milling cutter

The internal disc milling cutter consists of six repeating sets on each of its side. Each set, in turn, contains three cassettes equipped with single cutting inserts, i.e. there are 18 cassettes in total on one side of the disc milling cutter (36 on the both sides).

The cassettes with mounted cutting inserts are positioned in the body tangentially to the circle with diameter  $31.10^{\pm 0.05}$  mm. In each set, the first two cassettes are equipped with E-type cutting inserts to machining cylindrical surface of the crankpin, while the third cassette – is equipped with S-type cutting insert to machining transition radius area and web of crank, connecting crankpin with the main journal. For instance, the Figure 4 shows view of two sets of cassettes with cutting inserts from both sides of the body of the internal disc milling cutter. In addition, on the edges of E-type inserts, which are milling cylindrical surface of the crankpin, numbers of planes  $p$ , for which the calculations were carried out in the model, were marked.

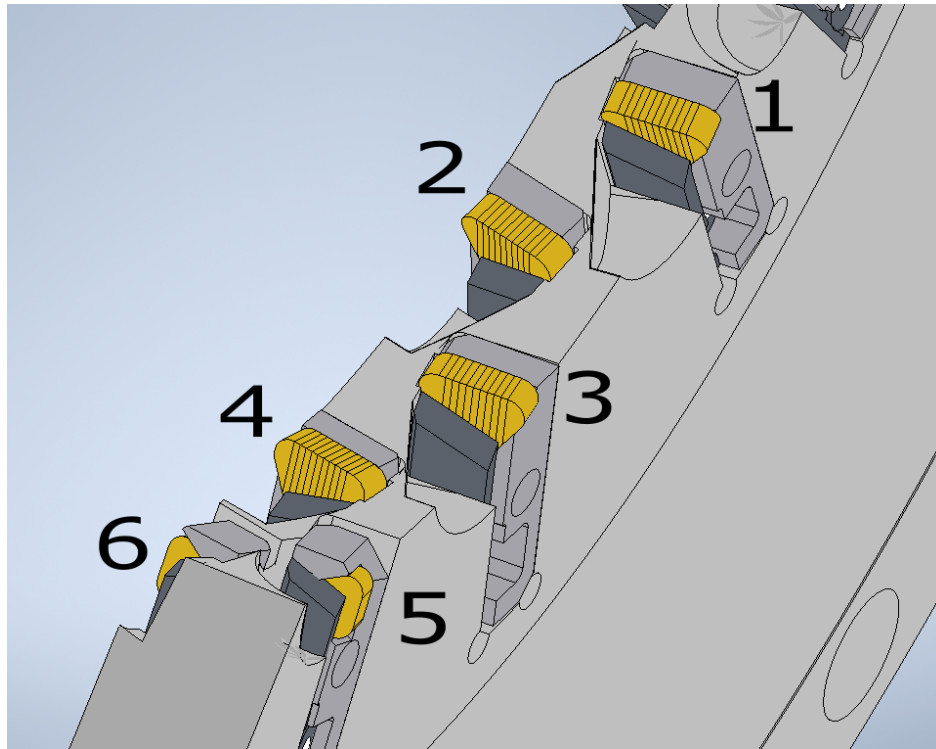


Fig. 4. Two sets of cassettes from the both sides of the body of the internal disc milling cutter: 1;3;5, and 2;4;6, where 1,2,3 and 4 - E-type cutting inserts (27.A58 and 27.A59) shaping the cylindrical surface of the crankpin; 5 and 6 - S-type cutting inserts (27.A62 and 27.A66) shaping the transition radius and web of the crank

The machining cycle of a single crankpin consists of three operations:

- pushing with straight-line motion of the eccentric housing with internal disc milling cutter close to the standstill crankpin (or main journal) of the crankshaft, and indentation of the cutter into the crankpin into the required depth, (starting position),
- real machining cycle consisting of a single complete rotation of the eccentric housing with speed  $n_{om}$  with internal disc milling cutter rotating with  $n_{mc}$  around the axis of machined crankpin of the crankshaft,
- stoppage and retracting of the eccentric housing with a rotating internal disc milling cutter away from the crankpin, and positioning for machining of the next crankpin.

Modeling of the machining process was limited to the second operation, where the cylindrical surface of the milled crankshaft's crankpin, transition radius area, and web of the crank are shaped (the calculations were carried out for the shaping of the cylindrical surface of the crankpin only).

At the beginning of this operation (for the time  $t = 0$ ) position of cutting inserts of the set with number  $i = 0$  is defined by angle  $\alpha_0(t = 0)$ . Whereas, angular position  $\alpha_i(t = 0)$  of the cutting inserts for the remaining sets of cassettes around the circumference of the internal disc milling cutter is described by the following equation:

$$\alpha_i(t = 0) = \alpha_0(t = 0) + i \cdot 360^\circ / l_z, \quad i = 0, 1, \dots, l_z - 1 \quad (1)$$

where:  $l_z$  number of all sets of the cassettes with cutting inserts of internal disc milling cutter.

Modeling of the machining process, i.e., removal of successive layers of material, is connected with the calculation of the mutual location of cutting inserts in the set of cassettes and with the calculation of the axis of rotation of the spinning internal disc milling cutter at any moment of time  $t$  (Fig. 3). Because the rotational speed  $n_{mc}$  of the disc milling cutter is several dozen times higher than rotational speed  $n_{om}$  of the eccentric housing with rotating disc milling cutter, it has been assumed that angular position  $\alpha_0(t)$  of cutting inserts of the set of the cassettes with number  $i = 0$  of the disc milling cutter will be taken as the decisive variable.

Then, the angular position  $\varphi(t)$  of the eccentric housing, and at the same time, the axis of rotation of the rotating internal disc milling cutter will be given by the formula:

$$\varphi(t) = \frac{n_{om}}{n_{mc}} \cdot (\alpha_0(t) - \alpha_0(t=0)) \quad (2)$$

where:  $\alpha_0(t = 0)$  is starting angular position of cutting inserts of the set with number  $i = 0$  in moment of time  $t = 0$ , while  $n_{om} = v_f / 2\pi(r_{mc} - r_{ck})$ , whereas  $n_{mc} = v / 2\pi r_{mc}$ ,  $v$  – peripheral speed of the internal diameter of the disc cutter.

Moreover, a coordinate system has been assumed in which axis  $Y$  passes through the axis of the main journals and axis of the machined crankshaft's crankpin at the moment  $t = 0$  of duration of the second, main machining activity. On the other hand, intersection point of axis  $X$  of this system with axis  $Y$  at the moment  $t = 0$  coincides with starting position of the point  $M$  of the axis of the rotation of the internal disc milling cutter.

The position of cutting inserts of individual sets of the internal disc milling cutter on plane  $XY$  of the assumed coordinate system is connected with the position of the point  $M$  of the axis of rotation of the disc cutter. The coordinates of the point  $M = [X_M, Y_M]^T$  in the starting position are described by the dependencies (Figs. 3):

$$X_M=0, \quad Y_M=0 \quad (3)$$

while the clockwise displacement of the axis of rotation of the rotating internal disc cutter, with respect to the starting position, is described by the dependencies:

$$X_M=-U, \quad Y_M=V \quad (4)$$

where:  $U=(r_{mc}-r_{ck}) \sin \varphi(t)$ ,  $V=(r_{mc}-r_{ck}) (1-\cos \varphi(t))$



Coordinates of the contact point  $C = [X_C, Y_C]^T$  are calculated from the following dependencies:

$$X_C = r_{mc} \sin \varphi(t), \quad Y_C = r_{mc} \cos \varphi(t) \quad (5)$$

where:  $X_C$  – abscissa of the contact point  $C$  of the equivalent cylindrical surface of the internal disc milling cutter to the cylindrical surface of the crankpin,  $Y_C$  – ordinate of the contact point of the equivalent cylindrical surface of the internal disc milling cutter (Fig. 3).

The axis (center) of the cylindrical surface of the machined crankpin  $P = [X_P, Y_P]$  does not change, and hence its coordinates are as below:

$$X_P = 0, \quad Y_P = r_{mc} - r_{ck} \quad (6)$$

Calculations of the coordinates of points on the surface of the crankpin, generated as a result of the movement of the tool, were carried out in selected cross-sections of the internal disc milling cutter. It has been assumed, that on width  $B$  of the disc cutter,  $p$  parallel cross-sections uniformly spaced will be analysed (Fig. 5). Planes of these sections intersect edges of cutting inserts of the cassettes located on both the sides of the housing of internal disc milling cutter in  $l_p$  points (Fig. 5). Hence, work of the edges of cutting inserts within a set of the points  $T_{ij}$  ( $i = 0, 1, \dots, l_z - 1; j = 1, 2, \dots, l_p$ ), located at the intersection of the edges of cutting inserts with planes of cross-sections of the internal disc milling cutter, was analysed for all its cassettes with inserts of  $E$ -type.

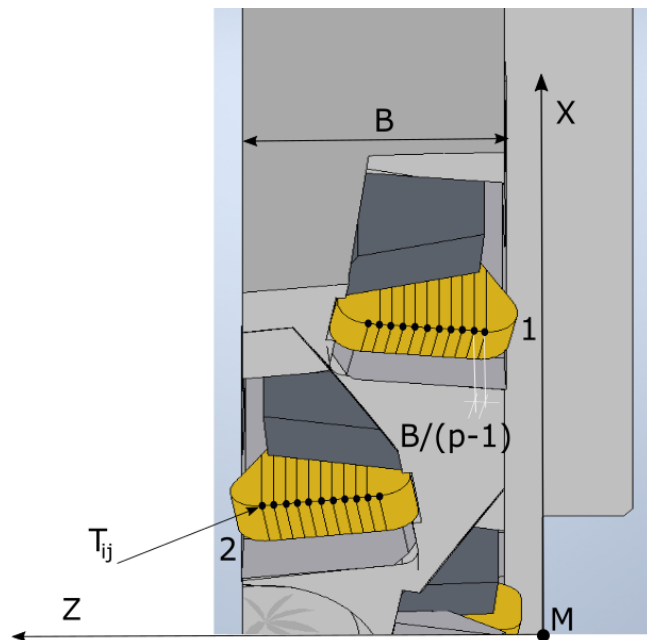


Fig. 5. Analysed cross-section planes of the internal disc milling cutter, 1;2 – E-type cutting insert, shaping cylindrical surface of the crankpin, 5 – S-type cutting insert, shaping transition radius and web of crank

In the Figure 3 location of the  $j$ -th point  $T_{ij}=[X_T, Y_T]^T$  on the edge of cutting insert of  $i$ -th cassette of internal disc milling cutter in moment of time  $t$  is described by the equations:

$$X_T=X_M+r_{mc} \cdot \cos\alpha_i(t), \quad Y_T=Y_M+r_{mc} \cdot \sin\alpha_i(t), \quad (8)$$

what enables modeling of the geometric shape of the crankpin after rough milling or shaping milling.

Finally, the model of the surface of the machined crankpin results from the mutual locations of analysed set of points at the edges of cutting inserts relative to the machined crankpin of the crankshaft. For instance, Figure 6 shows the determined trajectory of motion for a selected point on the edge of the cutting insert during the shaping of the cylindrical surface of the crankpin.

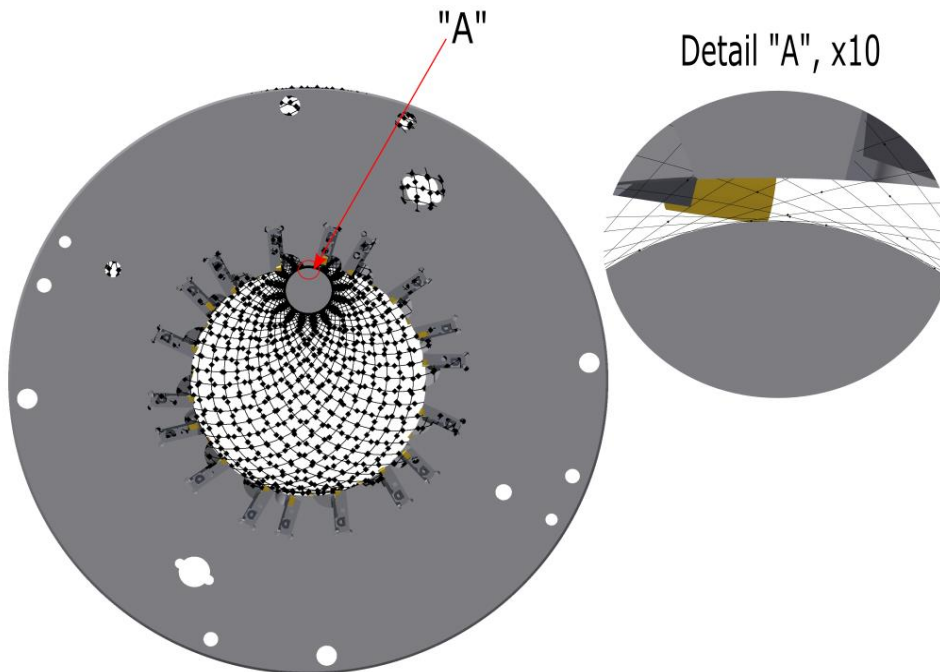


Fig. 6. Trajectory of motion of a selected point of the edge of the cutting insert during shaping of the surface of machined crankpin

#### 4. RESULTS OF THE STUDY AND THEIR ANALYSIS

In the study, one analysed simulation of the machining of the first crankpin from the flywheel side of the 4C90 diesel engine's crankshaft with four cranks mounted in a delivery vans. The geometry of machined crankpins is determined by diameter  $2r_{ck}=55.8$  (finished crankpin 55h6) mm and crank radius  $r_w=47.5^{\pm 0.1}$  mm. The equivalent cylindrical surface of the internal disc milling cutter has a diameter  $2r_{mc}=280$ mm. The internal disc milling cutter is equipped on its perimeter from the both sides with  $l_z=2 \times 6$  sets of cassettes, whereas each of them consists of 3 cassettes with mounted cutting inserts. The denomination of individual inserts and their geometry in the working system are as follows: 27.A58 and 27.A59 -  $\alpha_{ne} = 5^\circ$ ,  $\gamma_{ne} = -5^\circ$   $\lambda_{ne} = 10^\circ$ ; while the inserts 27.A62 and 27. A66 participates in the machining of parts of the side surfaces of the crank only. The width of the internal disc milling cutter is 33 mm, whereas only its portion of 25 mm, which machines the cylindrical surface of the crankpin without a radial transition area, was taken into consideration. The width of the internal disc

milling cutter, which machines the crankpin on the length  $B=25$  mm, and its division to  $p=21$  cross-sections by planes perpendicular to the axis of the crankpin, spaced uniformly every 1.25 mm (Fig. 5), were taken into account in the analysis. As a result of the assumed division, it has been obtained  $l_p=21$  points on the edges of cutting inserts, as depicted in Fig. 5 with the use of dots.

From industrial practice, it is seen that the optimal cutting speed in the case of planetary milling of crankshaft crankpins with four cranks, made of 42CrMo4 steel, equals 110 m/min. Based on this, the rotational speed of the internal disc milling cutter has been calculated, which was considered a constant value  $n_{mc}=125$  rpm, for which the peripheral speed amounts to 109.95565 m/min (cutting speed  $v_c$  is a little bit lower with the value of the circular feed rate because we are dealing with down milling).

During the study, the influence of circular feedrate  $v_f$  of the axis of rotation of the internal disc milling cutter on the geometric shape of the surface of the crankpin after rough milling was analysed. The radius of the cylindrical surfaces of the crankpin, equal to  $r_{ck}=27.9$ mm, and crank radius equal to  $r_w=47.5^{±0.1}$  were considered in the calculations. The modeling was performed for each of the 21 cross-sections cut by planes perpendicular to the axis of the crankpin. The following values of the circular feed rate of the axis of rotation of the internal disc milling cutter were taken into account in the calculations:  $v_f = 1200; 2100; 3000$  mm/min. To ensure suitably high accuracy of the model, the angular position of the internal disc milling cutter was changed in the course of the calculations every  $1^\circ$ . As a result, 360 radii  $r_{ck}$  of machined crankpin have been obtained in each cross-section, which were used to construct the outlines of the roundness. To assess the outlines of the roundness generated in such a way, deviations of the roundness  $\Delta r_{ck}$ , as the largest distances of the points of outline of the virtual workpiece, being the sum of the highest peak and the deepest dale of the profile, have been determined. For this purpose, the average circle (reference one – LSC), the smallest circumscribed circle (MCC) and the biggest inscribed circle (MIC) have been determined for each outline of the roundness [15, 16]. Values of the roundness deviations  $\Delta r_{ck}$  of the crankpin in cases of circular feed rate  $v_f = 1200$  mm/min, in individual cross-sections, are included within interval  $0.0009 \div 0.0031$  mm, while in case of circular feed rate  $v_f=2100$  mm/min, these are included within interval  $0.0041 \div 0.0249$  mm, and for circular feed rate  $v_f=3000$  mm/min – these are  $0.0081 \div 0.0759$  mm. The differences result from different radii  $r_{mc0j}$  of individual points on the edges of the cutting inserts of the internal disc milling cutter.

Example results of modeling of the outline of the roundness of the crankpin in cross-section cut by plane  $Z_9=10.0$  mm, for three values of circular feed rate, are presented in the Fig. 7, where the average circle (LSC) was additionally marked with a thin line [1, 12]. Whereas, calculated from the model values of the radii of the crankpin for the average circle (reference one), determined using the least squares method  $r_{ck LSC}$ , value of the smallest circumscribed circle (MCC)  $r_{ck MCC}$ , value of the biggest inscribed circle (MIC)  $r_{ck MIC}$ , and value of deviation of the roundness  $\Delta r_{ck}$  [12-14], have been specified in the Table 1. Together with increasing circular feed rate of the axis of rotation of internal disc milling cutter, value of radius of the biggest inscribed circle  $r_{ck MIC}$  almost does not change (increases with  $1.1 \mu\text{m}$ ), while value of the radius of the smallest circumscribed circle  $r_{ck MCC}$  increases significantly (increase with  $11.7 \mu\text{m}$ ). From the Fig. 7 it is also possible to see, that with an increase in circular feed rate, the peaks, which are the result of a more and more prolonged temporary lack of contact between the cutting inserts of individual sets of the cassettes and the machined crankpin, begin to be more enhanced.

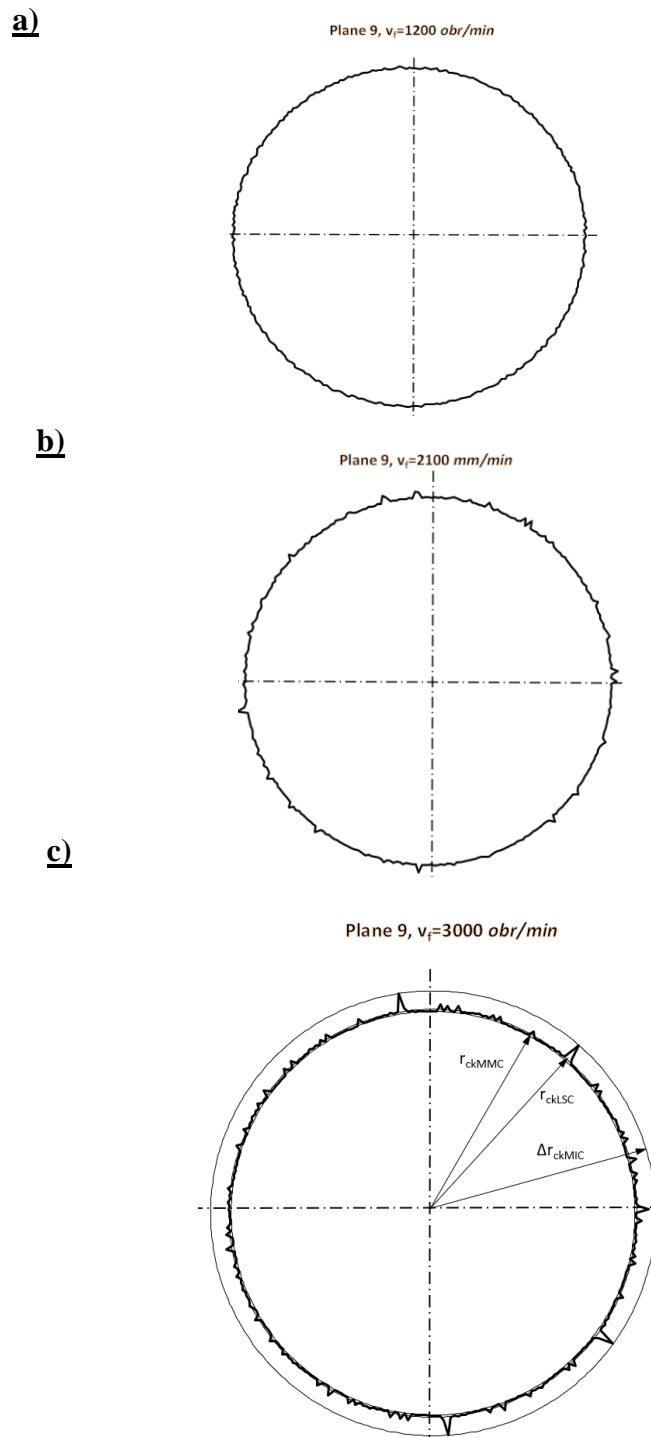


Fig. 7. Outline of the roundness and average circle (reference one) in cross-section cut by plane  $Z_9=10.0 \text{ mm}$  of the crankpin after rough machining for different values of circular feed rate – 1200 mm/min; b – 2100 mm/min; c – 3000 mm/min; magnification of the deviation in relation to the reference circle amounts to  $200\times$

Tab. 1

Values of the reference circle radii  $r_{ck\ LSC}$ , values of the smallest circumscribed circle  $r_{ck\ MCC}$ , the biggest inscribed circle  $r_{ck\ MIC}$ , and values of the roundness deviation  $\Delta r_{ck}$  of the crankpin for constant rotational speed of the internal disc milling cutter  $n_{mc}$  and variable value of circular feed rate  $v_f$  in the cross-section cut by plane  $Z_9=10.0$  mm

$v_f$ , mm/min	$r_{ck\ LSC}$ , mm	$r_{ck\ MCC}$ , mm	$r_{ck\ MIC}$ , mm	$\Delta r_{ck}$ , mm
1200	27.6988	27.6995	27.6982	0.0013
2100	27.6999	27.7048	27.6995	0.0053
3000	27.7003	27.7076	37.6995	0.0081

A particularly useful parameter, called cylindricity deviation and denoted in practice as  $CYL_t$ , was adapted to assessment of outlines of the cylindricity [1, 12]. According to the PN-EN ISO 1101:2006 standard, this is a sum of the biggest positive and absolute value of the smallest negative local deviation of the cylindricity, measured relative to the associated cylinder, determined with use of the least square method.

To determine and evaluate the outlines of the cylindricity of the surface of the crankpin machined with planetary milling, a strategy of outlines of roundness was implemented, consisting of collecting points on the circumference of the series of mutually parallel cross-sections cut by planes perpendicular to the axis of the workpiece [12-14].

In the Fig. 8 are presented outlines of the cylindricity of surface of the crankpin, obtained on the basis of the geometrical model for three values of circular feed rate  $v_f$ . The deviation of cylindricity of the crankpin, determined from the model for circular feed rate value  $v_f=1200$  mm/min amounted to  $CYLr_{ck}=0.2272$  mm, while for value of circular feed rate  $v_f=2100$  mm/min, -  $CYLr_{ck}=0.2406$  mm, and for value of circular feed rate  $v_f=3000$  mm/min, -  $CYLr_{ck}=0.2929$  mm. As can be seen, the cylindricity deviation of the crankpin distinctly increases with an increase in circular feed rate. This can be explained by the fact that the workpiece is not a cylinder but a prism with a regular polygon base. The sides of this polygon are not segments of a straight line, but arcs with a radius corresponding to the radius of the circle tangent to the edges of cutting inserts of the internal disc milling cutter. These differences result from the fact that the number of sides of the polygon of the machined workpiece decreases with an increase in the value of the circular feed rate of the axis of rotation of the internal disc milling cutter, and thus the distance of the inscribed circle from the intersection point of adjacent sides of the polygon increases.

In the next step, the outline of the cylindricity of the surface of the crankpins, obtained on the basis of the geometrical model, was longitudinally intersected by planes passing through the axis of the cylinder for the angles  $0^\circ$ ;  $90^\circ$ ;  $180^\circ$  and  $270^\circ$ . The intersections were made for the outline of the cylindricity of the surface of the crankpins obtained for a constant value of rotational speed of the internal disc milling cutter  $n_{mc} = 125$  rpm, and values of circular feed rate  $v_f=1200$ ; 2100 and 3000 mm/min. Calculations of the value of the radius  $r_{ck}$  of outline (generatrix) of the cylindricity of the surface of the crankpins were performed for 21 cross-sections at intervals 1.25 mm. For instance, in the Fig. 8, an outline of the generatrix of the crankpin for three values of circular feed rate  $v_f=1200$ ; 2100 and 3000 mm/min, and an angular position of  $90^\circ$ . In addition, with lines of different colors, are marked the the radii of the reference cylinder of the smallest zone  $r_{ck\ MZCY}$  and radius of the circumscribed cylinder, and the radius of the inscribed cylinder.

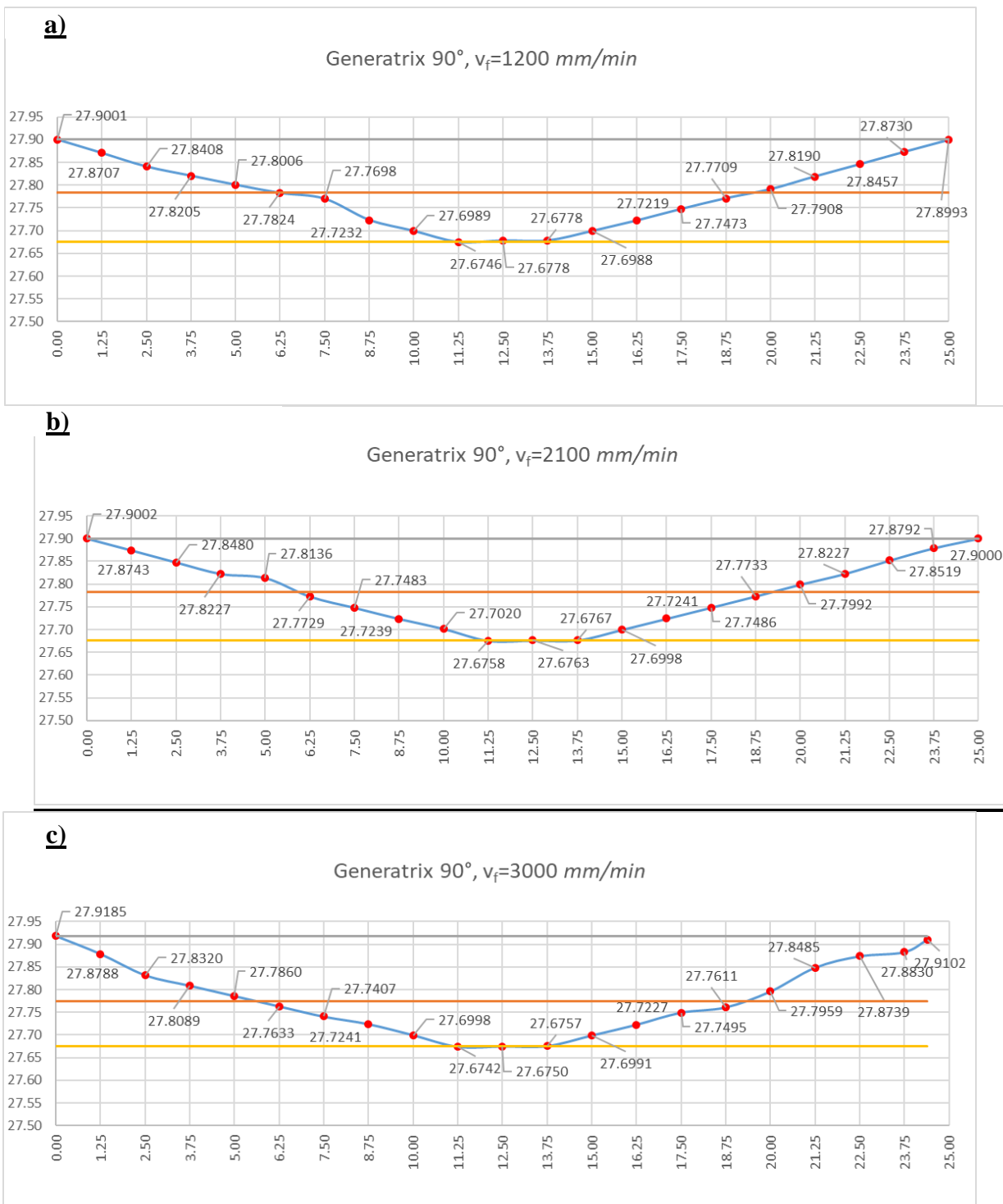


Fig. 8. Outline of generatrix of the crankpin for angular position 0° from the geometrical model (generatrix of the cylinder, radius of reference cylinder, radius of circumscribed cylinder, radius of inscribed cylinder):

- a) for value of circular feed rate  $v_f = 1200$  mm/min,
- b) for value of circular feed rate  $v_f = 2100$  mm/min,
- c) for value of circular feed rate  $v_f = 3000$  mm/min; magnification of the deviations relative to the reference cylinder amounts to 100×

#### 4. SUMMARY

Based on calculations carried out in selected planes of cross-sections of crankpins of the crankshaft with 4 cranks, after simulation of planetary milling with the use of an internal disc milling cutter, i.e., with cutting inserts directed inwards, it was found that:

- increase in the value of the circular feed rate of the axis of rotation of the internal disc milling cutter practically does not cause an increase in the value of the radius of the biggest inscribed circle  $r_{ckMIC}$ , while the value of the radius of the smallest inscribed circle  $r_{ckMCC}$  distinctly increases.
- values of deviations of the roundness  $\Delta r_{ck}$  for the crankpin after planetary milling with circular feed rate of the axis of rotation of the internal disc milling cutter of  $v_f = 1200$  mm/min are the smallest, and are included within interval  $0.0009 \div 0.0031$  mm, while for circular feed rate  $v_f = 2100$  mm/min - are bigger from 3,0 to about 11,86 times, and are included within interval  $0.0041 \div 0.0249$  mm, whereas for circular feed rate  $v_f = 3000$  mm/min they are bigger from 9.0 to about 24.5 times, and are included within interval  $0.0081 \div 0.0759$  mm in corresponding planes of the cross-sections.
- values of cylindricity deviation for the crankpin after planetary milling with a circular feed rate  $v_f = 1200$  mm/min amounted to  $CYLr_{ck} = 0.2272$  mm, while for value of circular feedrate  $v_f = 2100$  mm/min -  $CYLr_{ck} = 0.2406$  mm, and in case of circular feed rate  $v_f = 3000$  mm/min -  $CYLr_{ck} = 0.2929$  mm. As can be seen, deviation of the cylindricity of the crankpin distinctly increases together with increasing value of circular feed rate.

The simulation presented in this paper of the machining operation of the crankshaft's crankpins belongs to one of many examples of machining of a workpiece having complex shapes carried out on nc machine tools. The geometrical model presented in this paper can serve to develop an appropriate parametric machining program destined for other types of nc machine tools, as well as to make a preliminary selection of optimal machining parameters due to the value of machining allowances for grinding operations.

#### References

1. Adamczak Stanisław. 2009. *Pomiary geometryczne powierzchni. Zarysy kształtu, falistość i chropowatość*. Warszawa: WNT. ISBN: 978-8-3204-3526-9. [In Polish: Stanisław Adamczak. 2009. *Geometric measurements of surfaces. Shape outlines, waviness and roughness*. Warsaw: WNT. ISBN: 978-8-3204-3526-9].
2. Cichosz Piotr. *Narzędzia skrawające*. 2008. Warszawa: WNT. ISBN: 978-83-7926-08-2. [In Polish: Cichosz Piotr. *Cutting tools*. 2008. Warsaw: WNT. ISBN: 978-83-7926-08-2].
3. Czech Piotr. 2013. „Diagnosing a car engine fuel injectors' damage”. *Communications in Computer and Information Science* 395: 243-250. DOI: [https://doi.org/10.1007/978-3-642-41647-7\\_30](https://doi.org/10.1007/978-3-642-41647-7_30). Springer, Berlin, Heidelberg. ISBN: 978-3-642-41646-0; 978-3-642-41647-7. ISSN: 1865-0929. In: Mikulski Jerzy (eds), *Activities of transport telematics*, 13th International Conference on Transport Systems Telematics, Katowice Ustron, Poland, October 23-26, 2013.

4. Czech Piotr. 2012. „Identification of Leakages in the Inlet System of an Internal Combustion Engine with the Use of Wigner-Ville Transform and RBF Neural Networks”. *Communications in Computer and Information Science* 329: 175-182. DOI: [https://doi.org/10.1007/978-3-642-34050-5\\_47](https://doi.org/10.1007/978-3-642-34050-5_47). Springer, Berlin, Heidelberg. ISBN: 978-3-642-34049-9; 978-3-642-34050-5. ISSN: 1865-0929. In: Mikulski Jerzy (eds), *Telematics in the transport environment*, 12th International Conference on Transport Systems Telematics, Katowice Ustron, Poland, October 10-13, 2012.
5. Grzesik Wit. 2008. *Advanced Machining Processes of Metallic Materials. Theory. Modeling and Applications*. Amsterdam: Elsevier. ISBN: 978-0-0805-5749-6.
6. Grzesik Wit. 2007. „Toczenie styczne powierzchni obrotowych”. *Mechanik* 59(6): 257-263. ISSN: 0025-6552. [In Polish: Grzesik Wit. 2007. „Tangular turning of surfaces of revolution”. *Mechanic* 59(6): 257-263. ISSN: 0025-6552].
7. Materials: Heller Company.
8. Materials: Sandvik Coromant Company.
9. Materials: Steyr Company materials.
10. Materials: WFL Company materials.
11. Płonka Stanisław, Pytlak Bogusław, Placuch Krzysztof. 2013. „Modelowanie zgrubnego frezowania obrotowego czopów wałów korbowych”. *Mechanik* 86(12): 1021-1025. ISSN: 0025-6552. [In Polish: Płonka Stanisław, Pytlak Bogusław, Placuch Krzysztof. 2013. „Rough Rotary Milling Modeling of Crankshaft Journals”. *Mechanic* 86(12): 1021-1025. ISSN: 0025-6552].
12. PN-EN ISO 1101: 2006, *Tolerancje kształtu i położenia – Nazwy i określenia*. Warszawa: Polski Komitet Normalizacyjny. [In Polish: PN-EN ISO 1101: 2006, *Tolerances of shape and position - Names and definitions*. Warsaw: Polish Committee for Standardization].
13. PN-EN ISO 14660-1: 2001, *Specyfikacja geometrii wyrobów (GPS) – Elementy geometryczne. Część 1: Podstawowe terminy i definicje*. Warszawa: Polski Komitet Normalizacyjny. [In Polish: PN-EN ISO 14660-1: 2001, *Specification of product geometry (GPS) - Geometric elements. Part 1: Basic terms and definitions*. Warsaw: Polish Committee for Standardization].
14. PN-EN ISO 14660-2: 2001, *Specyfikacja geometrii wyrobów (GPS) – Elementy geometryczne. Część 2: Linia środkowa zaobserwowana walca i stożka, powierzchnia środkowa zaobserwowana, wymiar lokalny elementu zaobserwowanego*. Warszawa: Polski Komitet Normalizacyjny. [In Polish: PN-EN ISO 14660-2: 2001, *Specification of product geometry (GPS) - Geometric elements. Part 2: Observed Cylinder and Cone Centerline, Observed Center Surface, Observed Element Local Dimension*. Warsaw: Polish Committee for Standardization].
15. Rakowiecki Tadeusz, Skawiński Piotr, Siemiński Przemysław. 2011. „Wykorzystanie parametrów szablonów system 3D CAD do generowania modeli uzębień kół stożkowych”. *Mechanik* 84(12): 977-979. ISSN: 0025-6552. [In Polish: Rakowiecki Tadeusz, Piotr Skawinski, Przemysław Sieminski. 2011. „The use of 3D CAD template parameters to generate models of bevel gear teeth”. *Mechanic* 84(12): 977-979. ISSN: 0025-6552].
16. Skawiński Piotr, Siemiński Przemysław, Pomianowski Radosław. 2011. „Generowanie modeli bryłowych uzębień stożkowych za pomocą symulacji oprogramowanych w systemie 3D CAD”. *Mechanik* 84(11): 922-925. ISSN: 0025-6552. [In Polish: Skawinski Piotr, Przemysław Sieminski, Radosław Pomianowski. 2011. „Generation of solid models of bevel gears using simulations programmed in the 3D CAD system”. *Mechanic* 84(11): 922-925. ISSN: 0025-6552].



17. Wajand Jan. 2005. *Tłokowe silniki spalinowe średnio- i szybkoobrotowe*. Warszawa: WNT. ISBN: 83-204-3054-2. [In Polish: Wajand Jan. 2005. *Medium- and high-speed internal combustion piston engines*. Warsaw: WNT. ISBN: 83-204-3054-2].

Received 18.07.2023; accepted in revised form 22.09.2023



Scientific Journal of Silesian University of Technology. Series Transport is licensed under a Creative Commons Attribution 4.0 International License